Radio Frequency Measurements and Capacity Analysis for Industrial Indoor Environments

Yun Ai[1,2], Michael Cheffena[1], Qihao Li[1,2]
[1]Faculty of Technology, Economy and Management, Norwegian University of Science and Technology, Norway
[2]Faculty of Mathematics and Natural Sciences, University of Oslo, Norway
Email: {yun.ai, michael.cheffena, qihao.li}@ntnu.no

***Abstract*—In this study, path-loss and shadowing measurement results for three different industrial indoor environments at 900, 1600, and 2450 MHz are presented. The results show that the one-slope model fits the measured path-loss well, and the shadow fading samples follow a zero-mean Normal distribution. Low path-loss exponent values were found from our measurements, which may suggest the presence of heavy multi-path propagation in the measured channels. A comprehensive review of reported path-loss and shadowing measurements from various industrial environments is presented and compared with our measurement results. In addition, a channel capacity model with dependence on the measured parameters is investigated, which gives an insight to the effect of the propagation channel on system performance. This may assist the service providers to evaluate the technical feasibility of industrial wireless communications.**

***Index Terms*—Radio propagation, path-loss, shadowing, channel capacity, industrial environment.**

I. Introduction

In recent decades, there is a growing interest from the industry to deploy wireless sensor networks (WSNs) in factories. Wireless solutions have proven their advantages over wired systems in terms of deployment flexibility in various inaccessible or hazardous environments, and also the potential in data collection, enabling remote control, etc. However, industrial environments are often radio-harsh (e.g., high noise level, intensive interferences, shadowing, etc), which can possibly cause considerable impairments to mission-critical signals. Thus, an accurate knowledge about the industrial wireless channel is essential for the design and evaluation of robust wireless systems for industrial applications [1]–[3].

In this paper, we present measurement results conducted in typical industrial indoor environments at two most commonly used industrial, scientific and medical (ISM) frequency bands (900 and 2450 MHz) and a frequency in between the two bands (1600 MHz) [4]. The impact of the channel parameters on system performance is derived and discussed. In addition, a comprehensive review of reported measurements of path-loss and shadowing effects from various industrial environments is conducted and compared with our results. The obtained results should serve as a reference for implementation of WSN in industrial settings and future studies in relevant realms.

The paper begins in Section II by discussing the path-loss and shadowing propagation effects with a review on reported measurements in industrial environments. The measurement environments and set-up are described in Section III. In Section IV, the path-loss and shadowing measurement results are presented. The impact of channel parameters on the system capacity is derived and discussed in Section V. Section VI concludes the paper.

II. Related Work

A. Path-loss and shadowing effects

Path-loss occurs due to the attenuation of signal along the propagation path and is typically expressed as the ratio between the transmitted and received power. The path-loss (in dB) at transmitter (Tx) - receiver (Rx) distance d (in meters), $PL(d)$, can be expressed according to the one-slope model as:

$$PL(d) = PL(d_0) + 10\,n \cdot \log_{10}\Big(\frac{d}{d_0}\Big) + \chi_\sigma, \qquad (1)$$

where n is the path-loss exponent, which reflects the rate at which the received power decreases with distance. Parameter $PL(d_0)$ is the path-loss in dB at reference distance, d_0. There are two approaches to determine the intercept value of the path-loss at the reference point [5]:

1) fixed intercept approach: the intercept value is seen as a separate output of the least-square fitting;
2) non-fixed intercept approach: the intercept is chosen to be a fixed value and equal to the free space path-loss at the reference point according to the formula: $PL(d_0) = 20\log(4\pi/\lambda)$, where λ is the wavelength in meters.

Parameter χ_σ in (1) is a zero-mean Gaussian random variable with standard deviation σ when expressed in dB scale and represents the shadowing effect.

B. Overview of reported channel measurements

A number of indoor channel measurements in various industrial settings have been conducted over the years. In [2], measurements were done in industrial facility, where there existed both significant frequency selective and flat fading effects at 2.4 GHz. Path-loss exponent of 1.6 and 3.73 for line-of-single (LOS) and non-line-of-sight (NLOS) scenarios were found, respectively. From other three indoor industrial measurements under LOS scenario, path-loss exponent of 1.1 (for the chemical pulp and cable factories) and 1.86 (for nuclear power plant) were reported in [6]. The path-loss exponents for the chemical pulp and cable factories are lower than that in the nuclear power plant, which might be due to differences in scatterer type and density in the propagation environments.

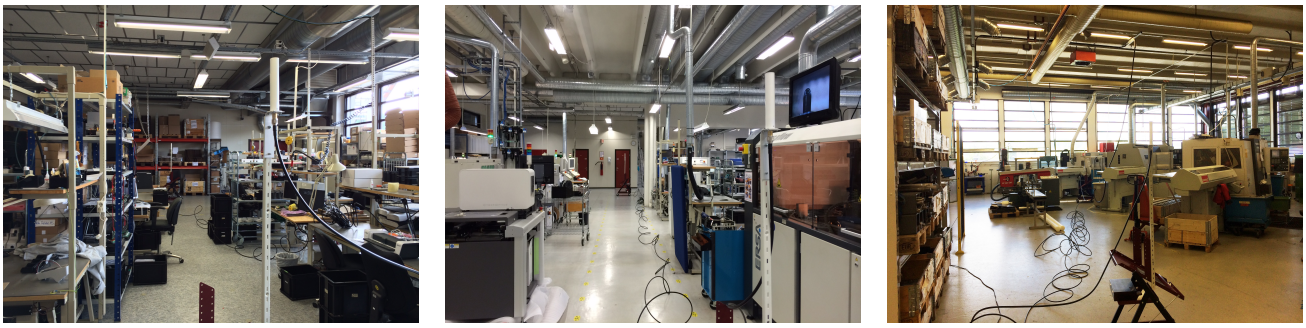

(a) Assembly room (b) Electronics room (c) Mechanical room

Fig. 1: Industrial measurement environments.

Luo *et al*. [7] reported path-loss measurements at 2.4 GHz and 5.8 GHz from a test-bed emulating an oil rig installation under both LOS and NLOS scenarios. Measurement results of excess path-loss from highly reflective environments (oil refinery and automobile assembly plant) for 25 MHz to 18 GHz signals were also reported in [8]. In [3], measurement results for various industrial topographies (at 900, 2400 and 5200 MHz) were reported with the introduction of a physical model explaining the dependency of one-slope model on the topography and frequency of the links. Furthermore, path-loss exponent measurements in electric power environments for smart grid applications were presented in [9].

Table I on the next page summarizes the aforementioned channel parameters (path-loss exponent n and shadowing standard deviation σ in (1)) from various industrial measurement campaigns. We can observe that the parameters vary significantly with the environment, frequency and link configuration.

III. Measurement Campaign

A. Environmental description

Observations from a large number of modern factories show that there are certain physical characteristics common to most industrial environments. Generally, industrial buildings are taller than ordinary office buildings and are sectioned into several working areas. Between the working areas, there usually exist straight aisles for passing people or materials. Modern factories usually have perimeter walls made of concrete or steel. The ceilings are often made of metal and supported with intricate metal supporting trusses. Besides the aforementioned common characteristics, the object type and density within specific environment may vary and play an important role in characterizing the propagation channel.

Propagation measurements presented in this paper were conducted in an electronics manufacturing factory in Gjøvik, Norway. The environments include an assembly shop, an electronics room and a mechanical room. The rooms share the aforementioned physical characteristics. The assembly shop is around 15 $\times$ 17 m^2 in size and about 5 meters in height. It houses two long work desks with three aisles along the longer dimension. Several big racks are placed along the aisle to place assembly components and a big metallic shelf holding manufacturing items is placed against the wall (see Fig. 1a). The electronics room is much bigger with an area of about 18 $\times$ 27 m^2 and a height of around 5 meters. It houses two rows of medium-size machinery with a lot of metallic valves present (see Fig. 1b). The mechanical room has a size of about 20$\times$30 m^2 with a height of around 6 meters. It has several big metallic machines but it is less occupied than the electronics room. Several pipes are placed off the roof and a big shelf holding manufacturing components is placed near the position of the Tx during the measurement campaign (see Fig. 1c).

B. Measurement set-up

Frequency-domain measurements were performed using a Rohde & Schwarz® ZNB Vector Network Analyzer (VNA). The VNA measures the frequency transfer function $H(f)$ directly by sweeping over the frequency band from 800 MHz to 2.7 GHz to cover the three frequencies of interest. Two omni-directional antennas with vertical polarization were connected to the VNA. Both the Tx and Rx were mounted on a telescopic mast of around 1.8 meters above the ground. The TX was injected with constant input power of -10 dBm and placed at a fixed position while the RX was moved following a straight trajectory, along which samples were taken at Tx-Rx distance from 2 to 16 meters with a step size of 0.5 meter. Altogether 25 measurements in each site were conducted to allow for the small-scale fading averaging.

IV. Measurement Results and Discussions

Table II shows measurement results of path-loss exponent n and shadowing standard deviation σ for each frequency and site discussed in Section III-A. Figure 2 displays an example of the path-loss measurement results in the assembly room. Linear regression is used to obtain the parameters n and σ from a set of measurement data $(10\log(d_i/d_0), PL_m(d_i))$ (only 3 sets of data for each frequency are shown in Fig. 2 while 25 data sets were used for the estimation). The measurement results in other rooms also show good agreement with the model and are not displayed here due to space limit.

The path-loss exponent n of all measurements are found to be lower than 2 (i.e., the path-loss exponent in free space), which may indicate the presence of heavy multi-path propagation in the channel. Smaller than 2 path-loss exponents have also been observed in various other measurement campaigns in industrial facilities (see Table I). It is also found that the

TABLE I: Reported path-loss and shadowing parameters in industrial environments

Environment type	**Frequency** (GHz)	**Propagation scenario**	n (-)	σ (dB)
Industrial facility [2]	2.40	LOS	1.60	-
		NLOS	5.00	-
Chemical pulp and cable factories [6]	2.45	LOS	1.10	-
Nuclear power plant [6]	2.45	LOS	1.86	-
Oil rig installation [7]	2.40	LOS	1.39	1.82
	5.80		1.76	1.83
	2.40	NLOS[1]	2.06	2.17
	5.80		2.44	2.45
	2.40	NLOS[2]	1.17	1.22
	5.80		1.41	1.31
Food and metal processing factories [3]	0.90	LOS[3]	3.51	7.70
		LOS[4]	2.49	7.35
	2.40	LOS[3]	3.44	8.63
		LOS[4]	2.16	8.13
	5.20	LOS[3]	2.59	6.09
		LOS[4]	0.91	4.79
500 Kv Substation [9]	2.40	LOS	2.42	3.12
		NLOS	3.51	2.95
Underground transformer vault [9]	2.40	LOS	1.45	2.45
		NLOS	3.15	3.19
Main power room [9]	2.40	LOS	1.64	3.29
		NLOS	2.38	2.25
Industrial facilities [10]	1.30	Mixed (LOS and NLOS)	2.20	7.90
Corridor [11]	1.90	LOS	1.80	-
Laboratory [11]	1.90	LOS	2.20	-
Industrial hall [11]	1.90	LOS	1.40	-

assembly room has the smallest path-loss exponents. This might be attributed to several factors. Firstly, the assembly room is much smaller than the other two rooms, creating a denser environment. The room is also filled with large numbers of small metallic structures. Both factors are likely to increase the number of reflections in the multipath profile, resulting in a less steep increase of path-loss with distance.

In our measurements, no clear relationship between path-loss exponent and frequency has been established. However, in reported measurements, various (even opposite) relationships between them have been observed. For instance, a decrease of the path-loss exponent with increasing frequency was found in wood processing and metal processing facilities in [3]. This decrease was explained by the fact that more objects act as reflectors when the wavelength decreases. Meanwhile, a proportional relationship between path-loss and frequency was seen in an oil rig installation [7], which might be due to different strengths of waveguide effect at different frequencies in the measured environment. The frequency dependent path-loss in industrial scenarios will be investigated as future work.

[1]The NLOS path-loss model uses the same $PL(d_0)$ as the LOS model.

[2]The NLOS path-loss model uses independent $PL(d_0)$.

[3]$PL(d_0)$ is determined with the fixed intercept approach as described in Section II.

[4]$PL(d_0)$ is determined with the non-fixed intercept approach as described in Section II.

TABLE II: Parameters of the one-slope model estimated from our measurements

Environment	f (MHz)	$PL(d_0)^3$ (dB)	n (-)	σ (dB)
Assembly room	900	25.0	1.72	3.80
	1600	32.5	1.37	2.58
	2450	35.5	1.69	3.93
Electronics room	900	26.0	1.96	2.29
	1600	33.5	1.83	3.48
	2450	35.0	1.81	2.29
Mechanical room	900	26.0	1.79	5.07
	1600	34.0	1.59	4.01
	2450	35.5	1.69	2.87

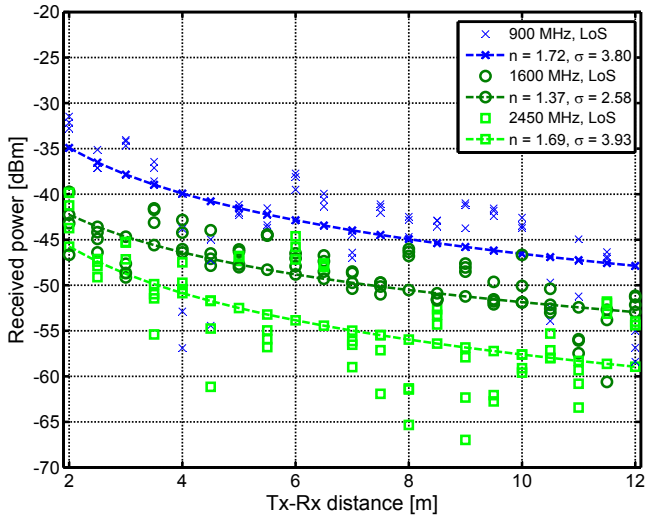

Fig. 2: Received power versus Tx-Rx distance at 0.9, 1.6 and 2.45 GHz for the assembly room.

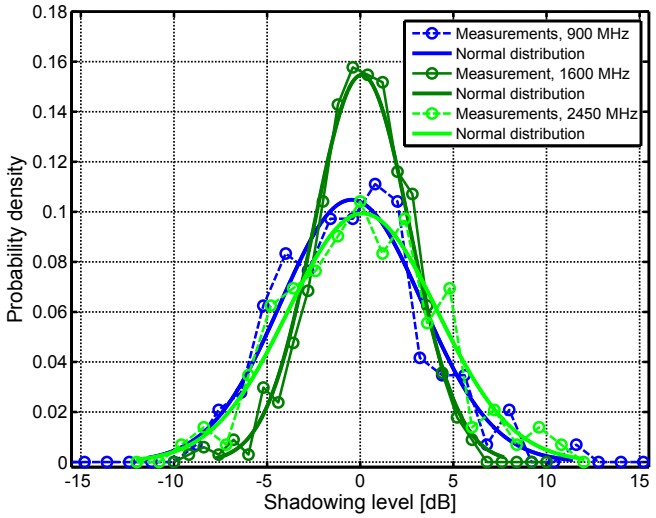

Fig. 3: Measured shadowing and Normal PDF at 0.9, 1.6 and 2.45 GHz for the assembly room.

The shadow fading samples of all the measurements were found to follow a zero-mean Normal distribution with probability density function (PDF) given by

$$f(\chi_\sigma) = \frac{1}{\sigma\sqrt{2\pi}} \exp\left(-\frac{\chi_\sigma^2}{2\sigma^2}\right), \tag{2}$$

where σ is the variance of the shadowing samples, χ_σ.

Figure 3 shows the comparison between the measured shadowing and Normal distribution at different frequencies in the assembly room, indicating good agreement between them. Similar results are also found for the other two sites.

V. Channel Capacity Analysis

The capacity of a channel with bandwidth B (Hz) is given by Shannon's theory as [12]

$$\frac{C}{B} = \log_2\left(1 + \frac{S}{N}\right), \tag{3}$$

where $\frac{C}{B}$ denotes the channel capacity per unit bandwidth and $\frac{S}{N}$ is the received signal-to-noise ratio (SNR). Usually, due to time-varying fading effects, the $\frac{S}{N}$ in (3) is a random variable with some distribution. This makes the channel capacity also a random variable and imposes a time-varying degradation on the system performance.

The received SNR can be further expressed in dB scale as

$$\begin{aligned}\left(\frac{S}{N}\right)_{dB} &= P_r - P_n = P_t - PL(d) - P_n \\ &= P_t - \left[PL(d_0) + 10\,n \cdot \log_{10}\left(\frac{d}{d_0}\right) + \chi_\sigma\right] - P_n,\end{aligned} \tag{4}$$

where P_t and P_r are the transmitted and received power in dB, respectively. Parameter P_n denotes the noise power in dB.

The relationship between the channel capacity and the channel parameters (e.g. path-loss exponent, shadowing deviation) at the Tx-Rx distance d can be obtained from:

$$\frac{C}{B} = \log_2\left(1 + 10^{\left(P_t - PL(d_0) - 10n\log_{10}(\frac{d}{d_0}) - \chi_\sigma - P_n\right)/10}\right). \tag{5}$$

The cumulative distribution function (CDF) of the channel capacity taking into account the path-loss and shadowing effect can be obtained by using (3) and (4):

$$\begin{aligned}F_{\frac{C}{B}}(y) &= \Pr\left[\frac{C}{B} \le y\right] = \Pr\left[\left(\frac{S}{N}\right)_{dB} \le \underbrace{10\log_{10}(2^y - 1)}_{f^{-1}(y)}\right] \\ &= \Pr\Big[\underbrace{P_t - PL(d_0) - 10\,n\log_{10}\left(\frac{d}{d_0}\right) - P_n - f^{-1}(y)}_{x} \le \chi_\sigma\Big],\end{aligned} \tag{6}$$

where y is defined as the channel capacity threshold.

Then, utilizing (2) in (6), we obtain the closed-form expression of the CDF of the time-varying channel capacity:

$$\begin{aligned}F_{\frac{C}{B}}(y) &= \Pr\left[\chi_\sigma \ge x\right] = \int_x^\infty f(\chi_\sigma)\, d\chi_\sigma \\ &= 1 - 0.5 \cdot \left[1 + \operatorname{erf}\left(\frac{x}{\sqrt{2}\sigma}\right)\right].\end{aligned} \tag{7}$$

The PDF of the channel capacity follows immediately from its relationship with CDF:

$$\begin{aligned}f_{\frac{C}{B}}(y) &= \frac{\mathrm{d}}{\mathrm{d}y} F_{\frac{C}{B}}(y) \\ &= \frac{10\,(\log_{10} 2)\, 2^y}{\sqrt{2\pi}\,(2^y - 1)\,\sigma} \mathrm{e}^{-\left[\frac{x}{\sqrt{2}\sigma}\right]^2}.\end{aligned} \tag{8}$$

In order to verify the model given by (7) and (8), we consider the channel information obtained from the assembly shop. For each Tx-Rx position pair of the same distance, the channel capacity can be computed from the measurements according to

$$\begin{aligned}\left(\frac{C}{B}\right)_m &= \log_2\left(1 + \frac{S}{N}(f,d)\right) \\ &= \log_2\left(1 + |H(f,d)|^2 \cdot \frac{S}{N}(f,d_0)\right),\end{aligned} \tag{9}$$

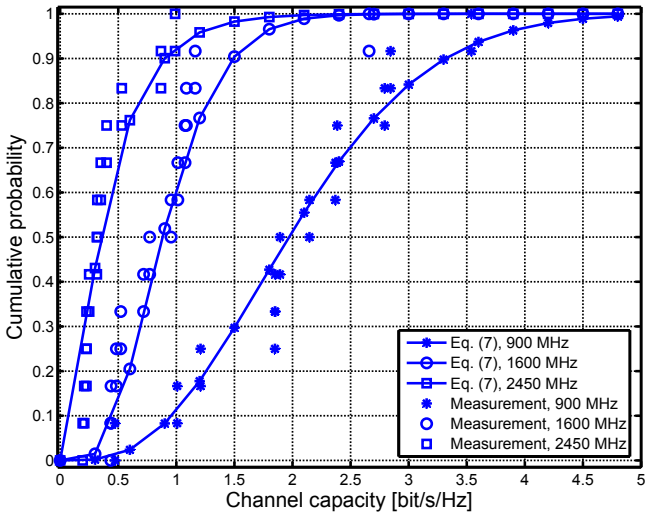

Fig. 4: CDF of theoretical channel capacity (eq. (7)) and measured capacity for the assembly room.

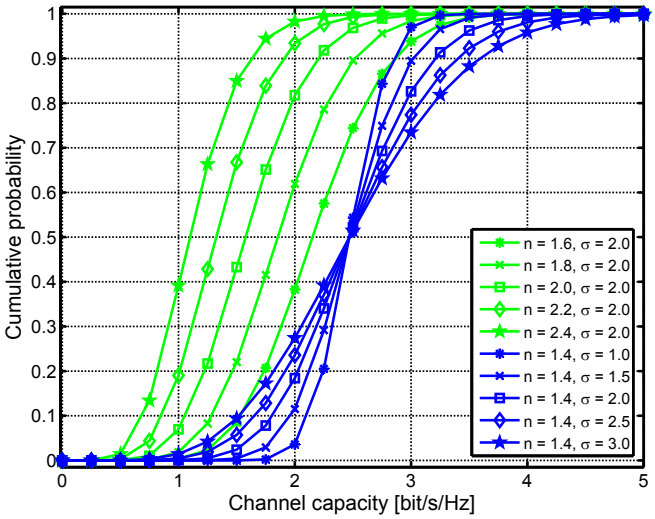

Fig. 5: Impact of the path-loss exponent and shadowing effect on the channel capacity.

where $\frac{S}{N}(f,d)$ is the SNR at the receiver at frequency f and Tx-Rx distance d. The parameter $\frac{S}{N}(f,d_0)$ is the SNR at the reference distance d_0.

Figure 4 shows the CDF of theoretical and measured channel capacity at Tx-Rx distance of 8 meters in the assembly room, which implies a good match between the theoretical model and measurements. The transmitted power is -10 dBm, noise level being -50 dBm and the other parameters are listed in Table II. The SNR at reference distance, $\frac{S}{N}(f,d_0)$ in (9), is set to be 15, 7.5 and 4.5 dB for 0.9, 1.6 and 2.45 GHz, respectively such that both capacities are equal at the reference distance d_0. These values are obtained by setting $\chi_\delta = 0$ and $d = d_0$ in (4). Figure 5 illustrates the impact of path-loss exponent and shadowing standard deviation on the CDF of the channel capacity at Tx-Rx distance of 8 meters with fixed input power (-10 dBm), noise level (-50 dBm) and $PL(d_0)$ (25 dBm). As expected, large path-loss exponent values degrades the channel capacity while large shadowing levels increase the variability of the channel capacity.

VI. Conclusion

Measurement results of path-loss and shadowing effects for three different industrial indoor environments at 900, 1600, and 2450 MHz were presented with a review of reported industrial channel measurement results. The measured path-loss was observed to fit the one-slope model well and the path-loss exponents lower than that of free space were observed, suggesting the presence of heavy multi-path propagation in industrial indoor environments. It was also shown that the shadowing fading fits the Normal distribution well.

The design of reliable communication systems for industrial applications requires link parameters such as throughput, availability and quality-of-service (QoS) to be determined and optimized with regard to the propagation channel. We thus derived and discussed the statistical properties of the channel capacity as functions of the channel parameters.

Acknowledgment

We gratefully acknowledge the Regional Research Fund of Norway (RFF) for supporting our research and Topro, Gjøvik for the support in the measurement campaign.

References

[1] E. Tanghe, D. Gaillot, M. Liénard, L. Martens, and W. Joseph, "Experimental analysis of dense multipath components in an industrial environment," *IEEE Transactions on Antennas and Propagation*, vol. 62, no. 7, pp. 3797–3805, 2014.

[2] D. Sexton, M. Mahony, M. Lapinski, and J. Werb, "Radio channel quality in industrial wireless sensor networks," in *Proc. of IEEE Sensors for Industry Conference*, 2005, pp. 88–94.

[3] E. Tanghe, W. Joseph, L. Verloock, L. Martens, H. Capoen, K. Van Herwegen, and W. Vantomme, "The industrial indoor channel: large-scale and temporal fading at 900, 2400, and 5200 MHz," *IEEE Transactions on Wireless Communications*, vol. 7, no. 7, pp. 2740–2751, 2008.

[4] IEEE 802 LAN/MAN Standards Committee and others, "Wireless LAN medium access control (MAC) and physical layer (PHY) specifications," *IEEE Standard*, vol. 802, no. 11, 1999.

[5] V. Erceg, L. J. Greenstein, S. Y. Tjandra, S. R. Parkoff, A. Gupta, B. Kulic, A. A. Julius, and R. Bianchi, "An empirically based path loss model for wireless channels in suburban environments," *IEEE Journal on Selected Areas in Communications*, pp. 1205–1211, 1999.

[6] S. Kjesbu and T. Brunsvik, "Radiowave propagation in industrial environments," in *Proc. of Annual Conference of the Industrial Electronics Society (IECON)*, vol. 4. IEEE, 2000, pp. 2425–2430.

[7] S. Luo, N. Polu, Z. Chen, and J. Slipp, "RF channel modeling of a WSN testbed for industrial environment," in *Proc. of IEEE Radio and Wireless Symposium (RWS)*, 2011, pp. 375–378.

[8] K. A. Remley, G. Koepke, C. Holloway, D. Camell, and C. Grosvenor, "Measurements in harsh RF propagation environments to support performance evaluation of wireless sensor networks," *Sensor Review*, vol. 29, no. 3, pp. 211–222, 2009.

[9] V. C. Gungor, B. Lu, and G. P. Hancke, "Opportunities and challenges of wireless sensor networks in smart grid," *IEEE Transactions on Industrial Electronics*, vol. 57, no. 10, pp. 3557–3564, 2010.

[10] T. S. Rappaport, "Characterization of UHF multipath radio channels in factory buildings," *IEEE Transactions on Antennas and Propagation*, vol. 37, no. 8, pp. 1058–1069, 1989.

[11] C. Oestges, D. Vanhoenacker-Janvier, and B. Clerckx, "Channel characterization of indoor wireless personal area networks," *IEEE Transactions on Antennas and Propagation*, vol. 54, pp. 3143–3150, 2006.

[12] M. El Khaled, P. Fortier, and M. Ammari, "A performance study of Line-of-Sight millimeter wave underground mine channel," *IEEE Antennas and Wireless Propagation Letters*, vol. 13, pp. 1148–1151, 2014.